

Structure and dynamics of self-organized neuronal network with an improved STDP rule

Rong Wang · Ying Wu · Li Wang ·
Mengmeng Du · Jiajia Li

Received: 3 August 2016 / Accepted: 9 January 2017 / Published online: 10 February 2017
© Springer Science+Business Media Dordrecht 2017

Abstract The chemical synapses in a neural network are known to be modulated by the neuronal firing activities through the spike-timing-dependent plasticity (STDP) rule. In this paper, we improve the multiplicative STDP rule by adding a momentum item with the aim of overcoming the low rate with which the neuronal network self-organizes into a stable complex structure. We find that the improved STDP rule with suitable momentum factors significantly speeds up the evolutionary process of the self-organized neuronal network. In addition, we explore the topological structure of self-organized neuronal network using complex network method. We show that the improved STDP rule generally results in a smaller node degree, clustering coefficient and modularity of self-organized neuronal network. Furthermore, we investigate the dynamical behaviors of self-organized neuronal network. We observe that depending on the momentum factor, the improved STDP rule has different effects on the network synchronization, neural information transmission, modularity and network complexity. Remarkably, for a specific momentum factor, the self-organized neuronal network shows the highest global efficiency

of information transmission and the best combination between functional segregation and integration, which reflects the optimal dynamics as well as the topological structure. Our results provide a reasonable and efficient modulating rule of chemical synapse underlying the neuronal firing activities.

Keywords STDP · Complex network method · Momentum item · Self-organized neuronal network

1 Introduction

The topological structures of neuronal network have received considerable attention in recent years due to their crucial roles for the dynamics of neural system such as the network synchronization and resonance [26,32]. The experimental findings have suggested the small-world and scale-free structures of neuronal network [14,16,36,39,43]. In addition, the global coupled network, random network and nearest-neighbor coupled network were also mathematically proposed to investigate the dynamical behaviors of neuronal network [13,24,25,29,47,50,51]. Recently, the self-organized structure was found to be more realistic to characterize the real neuronal network [45], and this type of structure with both small-world and scale-free properties has a great effect on the neuronal network dynamics [26,39,43]. For example, the self-organized neuronal networks have higher coherence resonance, stochastic resonance and efficiency in

R. Wang · Y. Wu (✉) · M. Du · J. Li
State Key Laboratory for Strength and Vibration of
Mechanical Structures, School of Aerospace, Xi'an
Jiaotong University, Xi'an 710049, China
e-mail: wying36@mail.xjtu.edu.cn

L. Wang
Faculty of Health, Medicine and Life Sciences,
Maastricht University, Maastricht, The Netherlands

information transmission compared to the global coupled network and random network [26]. Therefore, the exploration of self-organized neuronal network contributes to the more realistic understandings of structure and dynamics in the neural system.

The well-known feature of self-organized neuronal network is that the synaptic connections among neurons are controlled by the repeated firing activities of neurons [38,55,56]. This biological process is called the spike-timing-dependent plasticity (STDP) rule which has been found in various *vivo* and *vitro* experiments, such as the neocortical slices [33], rat hippocampal neurons [7], human motor system [6,10,54] and so forth [5,37,44]. The capability of STDP rule is updating the synaptic connections among neurons according to the relative timing between pre- and post-synaptic action potentials at a millisecond timescale. If the firing time for the presynaptic neuron is ahead of that for the postsynaptic neuron, the synaptic connection is strengthened; otherwise, it is weakened [34]. The updated synaptic connection again modulates the firing behavior of postsynaptic neuron and further affects the synaptic connection from postsynaptic neuron to presynaptic neuron. Apparently, the modulation of synaptic connection adaptively depends on the output of neurons, which in turn affects the neural responses. This feedback process between chemical synapses and neurons is believed to be closely related to the mechanisms of learning and memory in the brain [1,20,34]. Furthermore, the STDP rule has a great effect on the dynamics of neural system [1,26,55,57]. For example, in the absence of information transmission delay, the STDP rule can slightly depress the efficiency of network stochastic resonance [55] and induce the transition of spike propagation in neuronal networks [57]. Thus, investigating the effect of STDP rule on neural system is more helpful for revealing the mechanism of neural information transmission in the brain.

To date, there are two types of STDP rules [17,18,42,61]: an additive rule and a multiplicative rule. For the additive STDP rule, the modulated amount of synaptic weight is only decided by the difference between firing timings of pre- and postsynaptic neurons and is independent on the present synaptic weight [17]. But for the multiplicative STDP rule, the modulated amount of synaptic weight depends on both the neuronal firing timings and synaptic weight [17]. Although the two types of STDP rules can reflect the biological process, the multiplicative STDP rule

is more regarded as an improved version of additive STDP rule. More importantly, the multiplicative STDP rule results in a higher small-world property for self-organized neuronal network than the additive STDP rule, but it decreases the rate with which the neuronal network evolves into a complex small-world structure [18]. Consequently, the multiplicative STDP rule induces the higher efficiency of information transfer across the resulted neuronal network than the additive STDP rule, but it also brings the redundant feedback and decreases the modulating accuracy during the evolutionary process of neuronal network, which is accompanied by the higher energy cost for the biological system. Therefore, overcoming the low speed of multiplicative STDP rule may contribute to the less energy cost during the STDP biological process.

In this paper, we improve the multiplicative STDP rule with the aim of speeding up the convergence process and increasing the evolutionary accuracy of neuronal network. We first study the effect of improved STDP rule on the evolutionary process of self-organized neuronal network, and then we utilize the complex network method to explore the topological properties. Finally, we investigate the dynamical behaviors of self-organized neuronal network from the perspective of network synchronization, efficiency of information transmission and functional segregation and integration. We find that the improved STDP rule has a great effect on the evolutionary process, structure and dynamics of self-organized neuronal network. In particular, the improved STDP rule with a specific momentum factor results in an optimal neuronal network.

This paper is organized as follows. Section 2.1 provides a brief review of neuronal network model, Sect. 2.2 theoretically analyzes the advantages of the improved STDP rule compared to the multiplicative STDP rule, and Sect. 3 displays the results and Sect. 4 shows the discussion and conclusion.

2 Model

2.1 Neuronal network model

The neuronal network consisting of FitzHugh–Nagumo neurons is described as [9,11,26,49,60]:

$$\varepsilon \frac{dV_i}{dt} = V_i - V_i^3/3 - W_i + I_{\text{ext}} + I_i^{\text{syn}}$$

$$\frac{dW_i}{dt} = V_i + a + b_i W_i, \tag{1}$$

where V_i is the membrane potential of the i th neuron, W_i is the corresponding slow variable, and a, b_i and ε are the dimensionless parameters. I_{ext} is the applied current, I_i^{syn} is the total chemical synaptic current that the i th neuron receives and it obeys following equation:

$$I_i^{\text{syn}} = - \sum_j^N g_{ij} s_j (V_i - V_{\text{syn}}). \tag{2}$$

Here, g_{ij} is the synaptic weight from the j th neuron to the i th neuron and is updated by the STDP rule, s_j is the synaptic variable and satisfies:

$$\begin{aligned} \frac{ds_j}{dt} &= \alpha(V_j)(1 - s_j) - \beta s_j \\ \alpha(V_j) &= \alpha_0 / (1 + e^{-V_j/V_{\text{shp}}}), \end{aligned} \tag{3}$$

where $\alpha(V_j)$ is the synaptic recovery function and β is the rate of synaptic decay.

In Eq. (2), V_{syn} is the reversal potential of chemical synapse, which decides the classification of chemical synapse: excitatory synapse or inhibitory synapse. Here, the reversal potential for excitatory synapse is set as 0 mV, and it is equal to 2 mV for inhibitory synapse [26].

2.2 STDP rule

In the case that the presynaptic neuron i fires at the time t_i and the postsynaptic neuron j fires at t_j , the STDP updating function $F(\Delta t)$ is defined as [26]:

$$F(\Delta t) = \begin{cases} A_+ \exp(-\Delta t/\tau_+) & \text{if } \Delta t > 0 \\ -A_- \exp(\Delta t/\tau_-) & \text{if } \Delta t < 0 \\ 0 & \text{if } \Delta t = 0 \end{cases} \tag{4}$$

where $\Delta t = t_i - t_j$ is the firing time lag, τ_+ and τ_- are the temporal windows for synaptic refinement, and A_+ and A_- determine the maximum amount of synaptic update.

For the multiplicative STDP rule, the firing time lag Δt is measured within the temporal windows for synaptic refinement, and the synaptic update is performed once the temporal window is passed. We set the T as the updating time at which the corresponding synaptic weight is $g_{ij}(T)$ and the firing time lag is $\Delta t(T)$.

Thus the updating process of synaptic weight $g_{ij}(T)$ is modeled as:

$$\Delta g_{ij}(T) = g_{ij}(T + 1) - g_{ij}(T) = g_{ij}(T) F(\Delta t(T)), \tag{5}$$

where the $g_{ij}(T)$ is always restricted into the region $[0, g_{\text{max}}]$. If the j th neuron first fires at the temporal windows for synaptic refinement, the $\Delta t(T) > 0$ and the corresponding modulated amount of synaptic weight $\Delta g_{ij}(T)$ is greater than zero value such that the synapse from j th neuron to i th neuron is reinforced; otherwise, it is weakened.

Apparently, the multiplicative STDP rule ensures that the $\Delta g_{ij}(T)$ varies according to the neuronal firing activities and synaptic weight $g_{ij}(T)$. However, the feedback of neural signals may be affected by its previous activities such as the refractory period [4], and the amount of synaptic update also may be related to its previous update. Thus we assume that the $\Delta g_{ij}(T)$ is affected by its previous updated amount $\Delta g_{ij}(T - 1)$ and improve the multiplicative STDP rule as:

$$\Delta g_{ij}(T) = g_{ij}(T) F(\Delta t(T)) + \sigma \Delta g_{ij}(T - 1), \tag{6}$$

where $\sigma \Delta g_{ij}(T - 1)$ is called the momentum term, and σ is the momentum factor.

Now we analyze the advantages of improved STDP rule. While the neuronal network eventually achieves a stable state, the $\Delta t(T) \rightarrow 0$ and $g_{ij}(T) \approx g_{ij}^*$ where g_{ij}^* is the final stable value of synaptic weight from neuron j to neuron i . The process of synaptic weight $g_{ij}(T)$ converging to the stable value g_{ij}^* contains the following four cases:

First, we assume that the $\Delta t(T - 1) > 0$ happens at updating time $T - 1$ and the $\Delta g_{ij}(T - 1) > 0$:

Case 1. If the $\Delta t(T) > 0$ and $\Delta g_{ij}(T) > 0$, the synaptic weight $g_{ij}(T)$ is much less than the g_{ij}^* and needs to be further strengthened. The added momentum term $\sigma \Delta g_{ij}(T - 1) > 0$ contributes to the further increase in synaptic weight such that the convergence rate of synaptic weight is speeded up (see Fig. 1).

Case 2. If the $\Delta t(T) < 0$, $\Delta g_{ij}(T) < 0$, the synaptic weight $g_{ij}(T)$ just crossed the g_{ij}^* and needs to be decreased. At this moment, the $\Delta t(T)$ is very close to zero and the modulation amount of synaptic weight $\Delta g_{ij}(t)$ is small. The $g_{ij}(T)$ would show the slight oscillation around the g_{ij}^* , which ensures the $g_{ij}(T + 1)$ less than the g_{ij}^* . Therefore, the momentum term $\sigma \Delta g_{ij}(T - 1) > 0$ slows down the decrease in

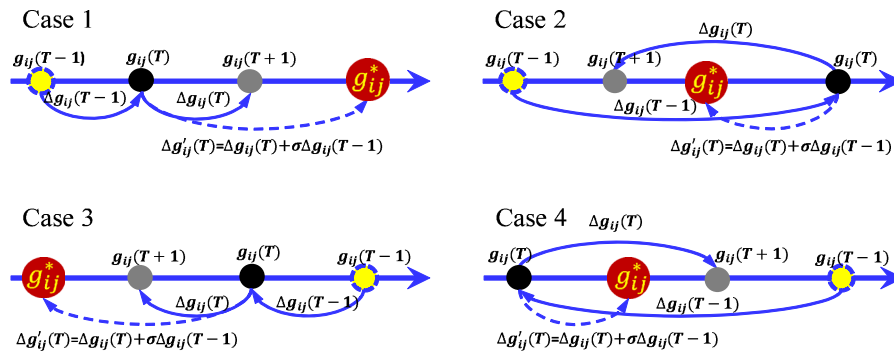


Fig. 1 The schematic diagram of comparison between the multiplicative STDP rule and the improved STDP rule. The horizontal axis represents the synaptic weight $g_{ij}(T)$ which increases along the direction of arrow. The solid curve indicates the direction of synaptic weight varying with updating time T for the multiplica-

tive STDP rule, and the dotted curve reflects the ideally updating process for the improved STDP rule. With the added momentum term, the improved STDP rule is more possible to promote the synaptic weight $g_{ij}(T)$ to converge to the stable value g_{ij}^*

synaptic weight to ensure the $g_{ij}(T + 1) \approx g_{ij}^*$, and thus the evolutionary accuracy is enhanced (see Fig. 1).

Second, we assume that the $\Delta t(T - 1) < 0$ happens at updating time $T - 1$ and the $\Delta g_{ij}(T - 1) < 0$:

Case 3. If the $\Delta t(T) < 0$, $\Delta g_{ij}(T) < 0$, the synaptic weight $g_{ij}(T)$ is far more than the g_{ij}^* and needs to be further decreased. The momentum term $\sigma \Delta g_{ij}(T - 1) < 0$ advances the decrease so that the $g_{ij}(T + 1)$ approaches to the g_{ij}^* more faster (see Fig. 1).

Case 4. If the $\Delta t(T) > 0$, $\Delta g_{ij}(T) > 0$, the synaptic weight $g_{ij}(T)$ is slightly less than the g_{ij}^* and needs to be strengthened. Due to the similar mechanism provided in Case 2, the momentum term $\sigma \Delta g_{ij}(T - 1) < 0$ decays the increase in synaptic weight so as to promote the $g_{ij}(T + 1)$ to converge to the g_{ij}^* more accurately (see Fig. 1).

It should be stressed that the momentum factor must not be less than zero value to guarantee the advantages of improved STDP rule, and it also must not be too big to ensure the $g_{ij}(T)$ accurately converging to the g_{ij}^* . The momentum factor is thus constricted into the region $(0, 1]$ according to the improved back propagation (BP) algorithm in the artificial neural network (ANN) where the momentum item is utilized to speed up the learning process [41]. Meanwhile, it also should be noted that the improved STDP rule is equivalent to the multiplicative STDP rule for the $\sigma = 0$, and the improved STDP rule would promote the synaptic weight $g_{ij}(T)$ rapidly and accurately to reach the stable value g_{ij}^* only for the suitable momentum factors.

The rest values of parameters utilized in above models are $\varepsilon = 0.08$, $I_{ext} = 0.1$, $a = 0.7$, $\alpha_0 = 2$, $\beta = 1$, $V_{shp} = 0.05$, $A_+ = 0.05$, $A_- = 0.0525$, $\tau_+ = \tau_- = 2$, $g_{max} = 0.1$ and b is uniformly distributed in $[0.45, 0.75]$. Furthermore, the initial conditions for all neurons are the same, that is $V = -1.2729$, $W = -0.5307$ and $s = 0.1172$.

3 Results

In this paper, the Euler–Maruyama algorithm is utilized to integrate the Eqs. (1–6) with a time step of 0.005 ms and a total time of 60 ms. The 50 excitatory neurons and 10 inhibitory neurons in a neuronal network are globally coupled by chemical synapse in the beginning, in which the autapse is not involved [26, 30, 31]. The synaptic weight is set as $g_{max}/2$ for the excitatory synapse, and it is equal to $3g_{max}/2$ for the inhibitory synapse. During the STDP modulating process, the weight of excitatory synapse is updated by the STDP rule, but it keeps consistence for the inhibitory synapse. Consequently, the global coupled neuronal network eventually evolves into a sparse directed weighted topological structure. Furthermore, for simplicity, the P_0 represents the proportion of synapse with weight in the range $[0, 0.1g_{max}]$ (weak coupling), the P_1 stands for the proportion of synapse with weight belonging to the region $[0.9g_{max}, g_{max}]$ (strong coupling), and the P_2 is responsible for the rest of occasions.

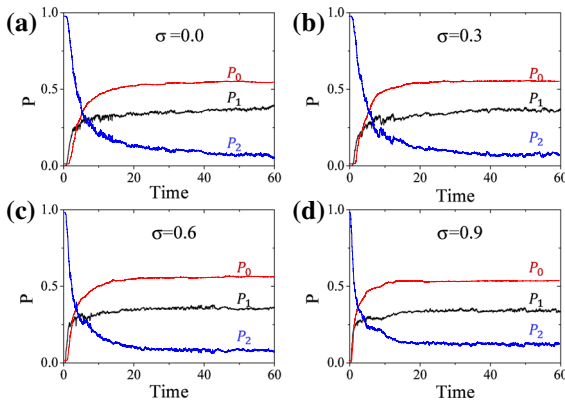


Fig. 2 The evolutionary process of P_0 , P_1 and P_2 for **a** $\sigma = 0.0$, **b** $\sigma = 0.3$, **c** $\sigma = 0.6$ and **d** $\sigma = 0.9$. Note that for the simulating time about over than 40 ms, the P_0 , P_1 and P_2 substantially keep stable as well as the neuronal network structure

3.1 Evolutionary process of neuronal network structure

In this part, we first investigate the evolutionary process of neuronal network structure with the modulation of multiplicative STDP rule ($\sigma = 0.0$) and improved STDP rule ($\sigma > 0$). Figure 2 shows the evolutionary process of P_0 , P_1 and P_2 for different momentum factors. As the evolutionary time increases, the P_2 decreases while

the P_0 and P_1 increase. This result indicates that during the evolutionary process, the competition between neurons strengthens a part of chemical synapses and weakens another, which is accompanied by the changes of topological structure of neuronal network. Meanwhile, the P_0 , P_1 and P_2 gradually reach the stable values, reflecting that the structure of neuronal network eventually achieves a stable state. More importantly, the P_0 , P_1 and P_2 for all momentum factors vary with a exponential form, revealing that the improved STDP rule has little effect on the evolutionary mode of neuronal network structure.

As discussed in Sect. 2.2, the improved STDP rule is excepted to speed up the evolutionary process of synaptic weight for the suitable momentum factors. To prove the theoretical analysis, the standard deviations (std) between P_0 , P_1 and P_2 are calculated to investigate the evolutionary rate of neuronal network. Figure 3 shows the evolutionary process of standard deviation for different momentum factors. As the evolutionary time increases, the standard deviations first decrease rapidly until the minimum values at which the P_0 , P_1 and P_2 curves intersect (see Fig. 2). Then, the standard deviations increase and eventually reach the relatively stable values, reflecting the stable topological structure of self-organized neuronal network. However, during

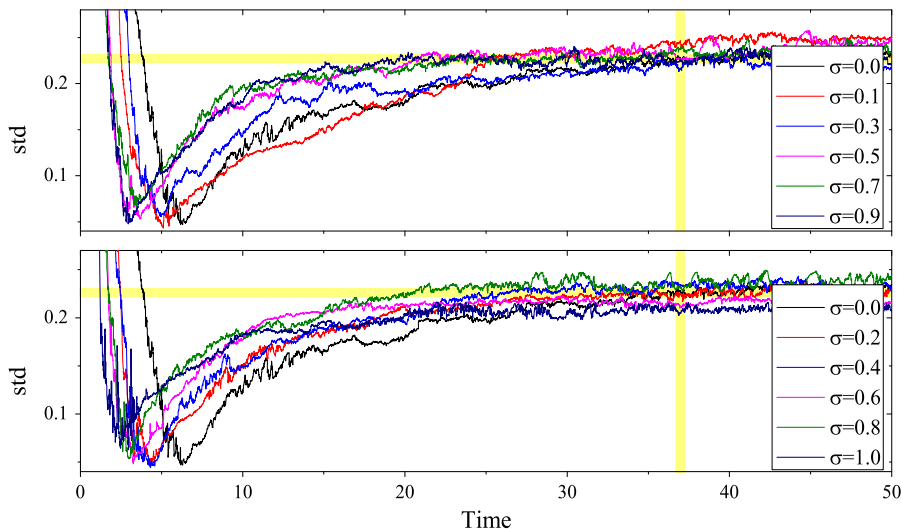


Fig. 3 The evolutionary process of standard deviation (std) between P_0 , P_1 and P_2 for different momentum factors. The horizontal yellow shadow indicates the relatively stable value of standard deviation for $\sigma = 0.0$, and the vertical yellow shadow means the start time at which the corresponding standard devia-

tion achieves the stable value. While the standard deviation for a momentum factor costs smaller time to achieve the relatively stable value, the corresponding neuronal network evolves into the self-organized structure with higher speed. (Color figure online)

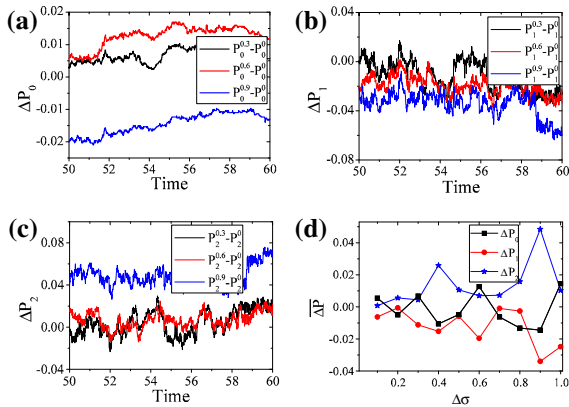


Fig. 4 The evolutionary process of **a** $\Delta P_0 = P_0^x - P_0^{0.0}$, **b** $\Delta P_1 = P_1^x - P_1^{0.0}$ and **c** $\Delta P_2 = P_2^x - P_2^{0.0}$, where $x = 0.3, 0.6, 0.9$, respectively. **d** The average values of ΔP_0 , ΔP_1 and ΔP_2 from 50 to 60 ms for different momentum factors

the evolutionary process, the standard deviations for $\sigma = 0.0-0.4$ are later to reach the stable values than those for the rest of momentum factors, indicating that the improved STDP rule indeed speeds up the evolutionary process of neuronal network for the suitable momentum factors such as $\sigma = 0.6, 0.9, 1.0$.

3.2 Topological structure of self-organized neuronal network

Due to the STDP modulation on the synaptic connections, the global coupled neuronal network eventually evolves into a sparse network and many neurons cluster together to form a module. The synaptic weight between neurons in the same module is strong, but it is relatively weak while the neurons are in different modules (see Fig. 6a, d and g). Consequently, a very large proportion of weak coupling and strong coupling exist in the self-organized neuronal network (see Fig. 2).

To investigate the differences between structures of self-organized neuronal network for different momentum factors, we calculated the differences $\Delta P_0 = P_0^\sigma - P_0^{0.0}$, $\Delta P_1 = P_1^\sigma - P_1^{0.0}$ and $\Delta P_2 = P_2^\sigma - P_2^{0.0}$ ($\sigma = 0.1, 0.2, \dots, 1.0$) from 50 to 60 ms during which the structures of neuronal network have achieved the stable states (see Fig. 2). Figure 4a shows the evolutionary process of ΔP_0 for $\sigma = 0.3, 0.6, 0.9$. The values of $P_0^{0.3} - P_0^{0.0}$ and $P_0^{0.6} - P_0^{0.0}$ are always larger than zero value, but not for $P_0^{0.9} - P_0^{0.0}$, reflecting that the improved STDP rule has dual effects on the P_0 .

Meanwhile, the values of ΔP_1 for $\sigma = 0.3, 0.6, 0.9$ are frequently smaller than zero value, and the $P_1^{0.3} - P_1^{0.0}$ has the minimum absolute value (see Fig. 4b), indicating that the improved STDP rule decreases the P_1 and this effect is relatively small for $\sigma = 0.3$. Furthermore, the value of ΔP_2 for $\sigma = 0.6, 0.9$ is generally larger than zero value, but the $P_2^{0.3} - P_2^{0.0}$ always fluctuates around the zero value (see Fig. 4c). This result reveals that the improved STDP rule increases the P_2 and this influence is relatively weak for $\sigma = 0.3$.

To further confirm the above results, we calculated the average values of ΔP_0 , ΔP_1 and ΔP_2 from 50 to 60 ms, the results are shown in Fig. 4d. As the momentum factor increases, the mean ΔP_0 fluctuates around the zero value, the mean ΔP_1 is frequently less than zero value and the mean ΔP_2 is always larger than zero value. Furthermore, these differences between P_0 , P_1 and P_2 for the improved STDP rule and the multiplicative STDP rule are statistically significant ($p < 0.05$ for all values of σ , two-sample T test). These results indicate that compared to the multiplicative STDP rule, the improved STDP rule significantly decreases the P_1 (strong coupling), increases the P_2 and has dual effects on the P_0 (weak coupling).

Above results have proved that the improved STDP rule has a great effect on the synaptic weight such that it would affect the topological structure of self-organized neuronal network. Hence, we introduced the complex network method to further investigate the effect of improved STDP rule on the topological structure. The definitions of complex network indices including the node degree, clustering coefficient and modularity in the directed weighted network are shown in ‘‘Appendix 1’’. We first calculated the complex network indices of self-organized neuronal network at time T_k where T_k varies from 50 to 60 ms with a step of 0.05 ms, and then averaged the complex network indices among the 201 neuronal networks as the mean value for each momentum factor.

The node degree measures the sparse degree of complex network, and the bigger value of node degree means the denser network. Figure 5a shows the mean node degree of self-organized neuronal network. As the momentum factor increases, the node degree gradually decreases, and these differences between node degree for the improved STDP rule and the multiplicative STDP rule are statistically significant ($p < 0.05$ for all values of σ , two-sample T test). This result indicates that the improved STDP rule induces the more

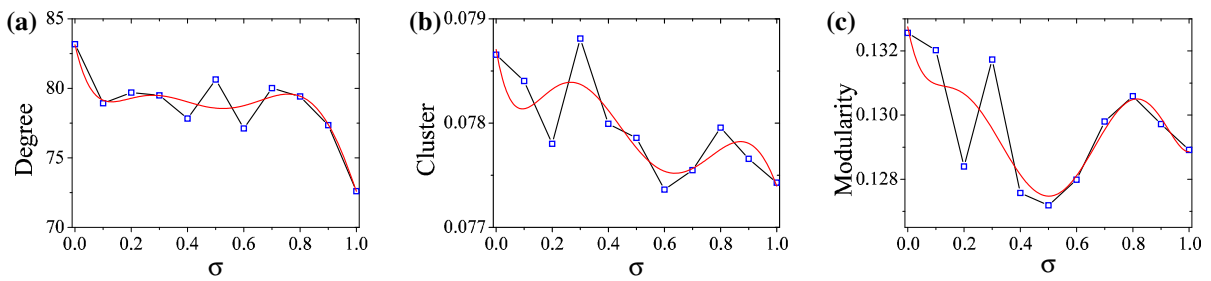


Fig. 5 **a** The node degree, **b** clustering coefficient and **c** modularity of self-organized neuronal network for different momentum factors. The red fitting lines reflect the changing trends of node

degree, clustering coefficient and modularity with the momentum factor increasing

sparse self-organized neuronal network than the multiplicative STDP rule.

The clustering coefficient measures the degree with which nodes tend to cluster together [28]. Figure 5b shows the mean clustering coefficient for different momentum factors. The clustering coefficient of self-organized neuronal network for $\sigma = 0.3$ is larger than that for $\sigma = 0.0$, but it is apparently decreased for the rest values of σ , among which the clustering coefficient is the smallest for $\sigma = 0.6$. More importantly, these differences between clustering coefficients of self-organized neuronal network for the improved STDP rule and the multiplicative STDP rule are statistically significant ($p < 0.05$ for all values of σ , two-sample T test). These results suggest that the improved STDP rule mostly decreases the mean clustering coefficient of self-organized neuronal network, and the decreased effect is the strongest for $\sigma = 0.6$.

The self-organized neuronal network exhibits the apparent modular structure (see Fig. 6a, d and g), the degree of which is measured by the modularity. As can be seen from Fig. 5c, the mean modularity of self-organized neuronal network for the improved STDP rule is significantly smaller than that for the multiplicative STDP rule, and the modularity for $\sigma = 0.5$ is the smallest. Furthermore, these differences between modularity for the improved STDP rule and the multiplicative STDP rule are statistically significant ($p < 0.05$ for all values of σ , two-sample T test). These results reveal that the improved STDP rule decreases the modular degree of self-organized neuronal network compared to the multiplicative STDP rule, and this decreased effect is the strongest for $\sigma = 0.5$.

Taken together, depending on the momentum factor, the improved STDP rule significantly changes the proportion of synaptic weight such that it generally results

in a more sparse, less clustered and modular topological structure of self-organized neuronal network.

3.3 Dynamics of self-organized neuronal network

The dynamics of complex network is closely related to its topological structure and even can be predicted by it [58]. Since the improved STDP rule has a great effect on the topological structure of self-organized neuronal network, the networks for different momentum factors are expected to exhibit apparently different dynamical behaviors. Therefore, we now investigate the dynamics of self-organized neuronal network. We firstly selected the neuronal network at the time T_k as the baseline network structure, in which the T_k varies from 50 to 60 ms with a step of 0.05 ms. Consequently, the 201 neuronal networks were obtained with the mostly same topological properties for each momentum factor. Based on the baseline network structures, we then again integrated the Eqs. (1–6) with a time step of 0.05 ms and a total time of 60 ms. Furthermore, we sampled the time series of firing activities of neurons from 30 to 60 ms and calculated the correlation coefficient between time series of neurons according to ‘‘Appendix 2’’. The correlation matrices were then obtained and regarded as the functional networks of self-organized neuronal network. Finally, based on the 201 functional networks for each momentum factor, we investigate the dynamics of self-organized neuronal network including the network synchronization, information efficiency and functional integration and segregation.

3.3.1 Network synchronization

The correlation coefficient (ρ) measures the phase synchronization between firing activities of neurons, where

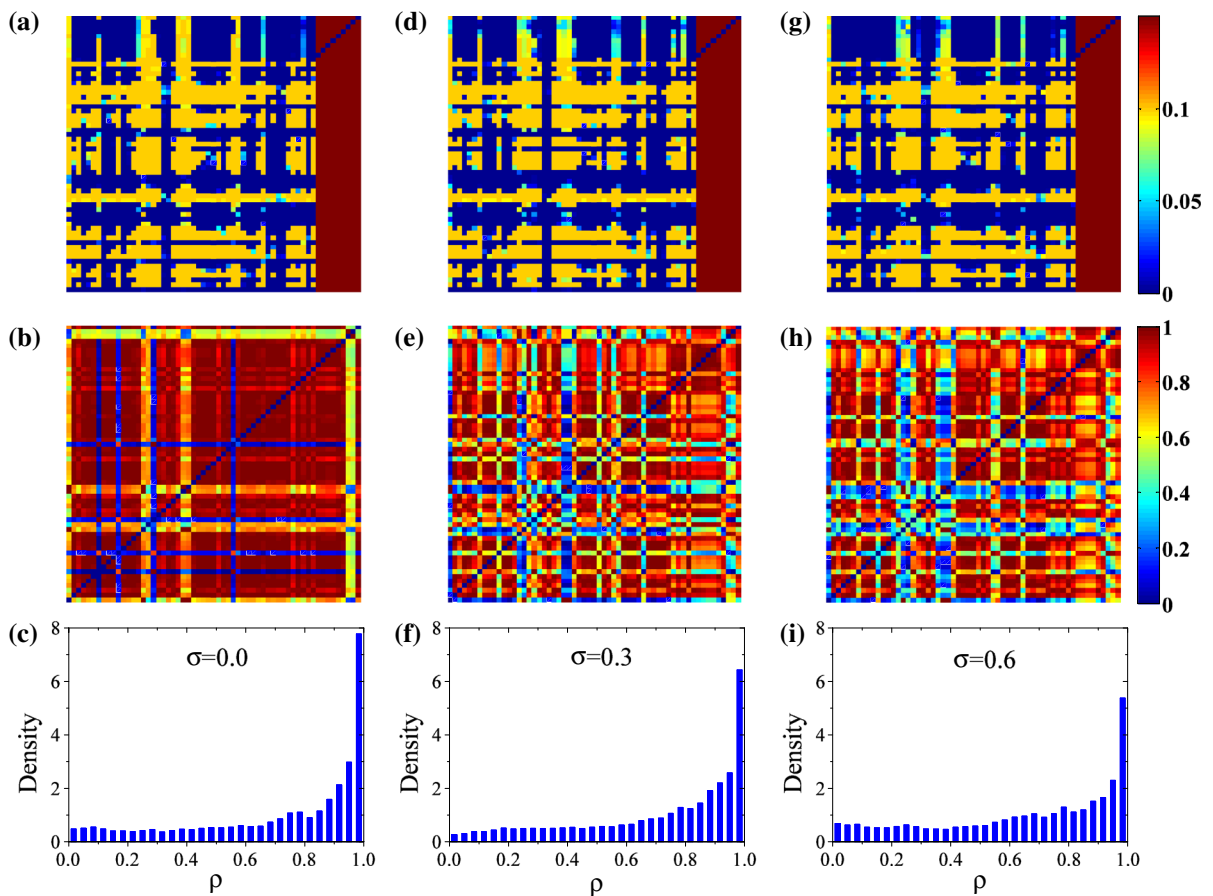


Fig. 6 The synaptic connection matrices of the self-organized neuronal networks at the time of 60 ms (*upper panel*), the corresponding functional networks (*middle panel*) and the probability

density distributions of absolute correlation coefficient (*lower panel*) for **a–c** $\sigma = 0.0$, **d–e** $\sigma = 0.3$ and **g–i** $\sigma = 0.6$

the $\rho = 1$ indicates the completely phase synchronization, and $\rho = -1$ reflects the completely anti-phase synchronization. Here we adopted the absolute correlation coefficient to characterize the firing synchronization among neurons. Figure 6c, f and i show the probability density distributions of correlation coefficient for $\sigma = 0.0, 0.3, 0.6$. The probability density of correlation coefficient has the largest value for $\rho \rightarrow 1$ and the smallest value for $\rho \rightarrow 0$, reflecting the strong synchronization among neurons in the self-organized networks. Moreover, the probability density for $\sigma = 0.0$ is obviously different from that for $\sigma = 0.3, 0.6$ with smaller probability density for $\rho \rightarrow 1$, indicating that the improved STDP rule may induce the smaller firing synchronization among neurons. Furthermore, we calculated the mean correlation coefficient to prove the

result. As seen in Fig. 7, the mean correlation coefficient exhibits the bimodal structure as the momentum factor increases. For a part of momentum factors such as $\sigma = 0.2, 0.9$, the mean correlation coefficient is significantly greater than that for $\sigma = 0.0$. But for the other part of momentum factors such as $\sigma = 0.6$, the mean correlation coefficient is apparently smaller than that for $\sigma = 0.0$. In addition, the mean correlation coefficient is the greatest for $\sigma = 0.2$ and is the smallest for $\sigma = 0.6$. More importantly, these differences between mean correlation correlation for the improved STDP rule and the multiplicative STDP rule are statistically significant except for $\sigma = 0.3$ ($p > 0.05$ for $\sigma = 0.3$ and $p < 0.05$ for the rest values of σ , two-sample T test). These results indicate that compared to the multiplicative STDP rule, the improved STDP rule con-

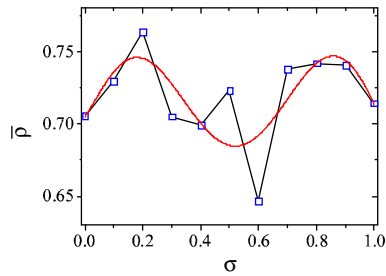


Fig. 7 The average value of absolute correlation coefficient of functional networks for different momentum factors. The *red fitting line* indicates the changing trend of average correlation coefficient with the momentum factor increasing

tributes to either strengthening the network synchronization or weakening it, and the strengthened effect is the strongest for $\sigma = 0.2$ and the weakened influence is the strongest for $\sigma = 0.6$.

3.3.2 Network efficiency

The neurons coupled together aims to communicate the neural information which apparently is related to the firing synchronization among neurons. Due to the great effect on the network synchronization, the improved STDP rule is expected to affect the neural information transmission across the network. To investigate the information transmission efficiency, we calculated the local information efficiency and global information efficiency of functional network, the definitions of which are seen in “Network efficiency” of Appendix 1.

The local efficiency measures the information transmission among sub-networks. As can be seen from Fig. 8a, the mean local efficiency of functional network for some momentum factors such as $\sigma = 0.2, 0.9$ is larger than that for $\sigma = 0.0$, but it is decreased for the other momentum factors such as $\sigma = 0.4, 0.6$. Meanwhile, these differences between local efficiency of functional networks for the improved STDP rule and the multiplicative STDP rule are statistically significant except for $\sigma = 0.3, 1.0$ ($p > 0.05$ for $\sigma = 0.3, 1.0$ and $p < 0.05$ for the rest values of σ , two-sample *T* test). These results reveal that depending on the momentum factor, the improved STDP rule either strengthens the local neural information transmission or weakens it. More importantly, the mean local efficiency of functional networks for $\sigma = 0.2$ is the biggest, indicating the strongest strengthened effect of improved STDP rule on local efficiency, and it is the smallest for

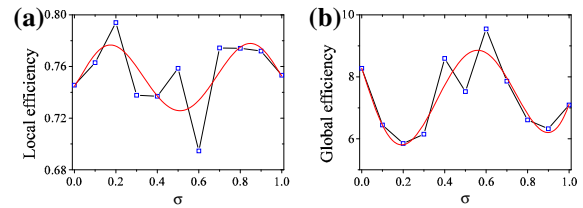


Fig. 8 **a** The local efficiency and **b** global efficiency of functional networks for different momentum factors. The *red fitting lines* reflect the changing trends of local efficiency and global efficiency as the momentum factor increases

$\sigma = 0.6$, revealing the strongest weakened influence. Furthermore, it should be noted that the evolutionary processes of average correlation and local efficient are similar as the momentum factor increases, reflecting that the local efficiency of information transmission is closely related to the synchronization within the local networks.

In contrary, the global efficiency characterizes the information flow across the global network. From Fig. 8b, the mean global efficiency of functional networks for $\sigma = 0.4, 0.6$ is larger than that for $\sigma = 0.0$, and the functional network for the rest of momentum factors has the decreased global efficiency. In addition, these differences between global efficiency for the improved STDP rule and the multiplicative STDP rule are statistically significant except for $\sigma = 0.4, 0.7$ ($p > 0.05$ for $\sigma = 0.4, 0.7$ and $p < 0.05$ for the rest values of σ , two-sample *T* test). These results reveal that the improved STDP rule has dual effects on the global efficiency: strengthening the global efficiency or decreasing it. More importantly, the global efficiency is the biggest for $\sigma = 0.6$, indicating the strongest effect on promoting the global neural information transmission, and it is the smallest for $\sigma = 0.2$, revealing the strongest weakened effect.

3.3.3 Network functional integration and segregation

As seen from Fig. 6b, e and h, the functional networks exhibit the apparent modular structure. The strong synchronization within the module is responsible to specific function in subsystems and results in a functional segregation, while the functional integration in charging of the information integration in global system needs strong synchronization between modules, which would wipe away the modular structure. The balance between functional segregation and integra-

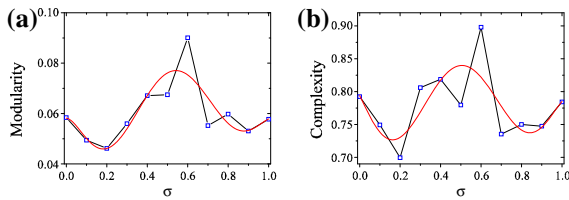


Fig. 9 **a** The modularity and **b** complexity of functional networks for different momentum factors. The *red fitting lines* indicate the changing trends of modularity and complexity as the momentum factor increases

tion is believed to be crucial for normal functioning of complex system, for example, the brain disorders often result from the imbalance between functional segregation and integration [59]. Furthermore, the network shows different synchronous patterns for different momentum factors (see Fig. 6c, f and i), which must affect the balance between functional segregation and integration. Therefore, we further investigate the functional integration and segregation of functional network using modularity and network complexity.

The modularity is a natural measure of modular degree and its definition is given in “Modularity” of Appendix 1. The larger the modularity, the more modular the network is and the stronger the functional segregation is [27]. Figure 9a shows the modularity of functional network for different momentum factors. The modularity increases for some specific momentum factors such as $\sigma = 0.6$ than that for $\sigma = 0.0$, but it is decreased for the other momentum factors such as $\sigma = 0.2, 0.9$. However, the statistically significant difference between modularity for the improved STDP rule and the multiplicative STDP rule mostly depends on the momentum factor ($p > 0.05$ for $\sigma = 0.3, 0.7, 0.8, 1.0$ and $p < 0.05$ for the rest values of σ , two-sample T test). These results reveal that the improved STDP rule has dual effects on the modularity: strengthening the functional segregation for $\sigma = 0.4–0.6$, and enhancing the functional integration for $\sigma = 0.1, 0.2, 0.9$. Furthermore, the modularity for $\sigma = 0.6$ is the largest, reflecting the strongest effect of improved STDP rule on functional segregation, and it has the smallest value for $\sigma = 0.2$, indicating the strongest influence on functional integration.

The network complexity S characterizes the balance between functional segregation, and integration [46, 59] and its definition is provided in “Appendix 3”. The S is closed to zero value for both nonsynchronous

and fully synchronous state, and the maximum complexity reflects the combination between functional segregation and integration [59]. From Fig. 9b, the network complexity nonlinearly varies as the momentum factor increases, during which the functional networks for some momentum factors such as $\sigma = 0.6$ have the larger complexity than that for $\sigma = 0.0$, but they have decreased complexity for another momentum factors such as $\sigma = 0.2, 0.9$. In addition, the two-sample T test provides the σ —dependent difference between complexity for the improved STDP rule and the multiplicative STDP rule ($p > 0.05$ for $\sigma = 0.3, 0.5, 1.0$ and $p < 0.05$ for the rest values of σ). Therefore, it is obvious that the improved STDP rule has the dual effects on the network complexity, decreasing the complexity for $\sigma = 0.1, 0.2, 0.7–0.9$ and increasing it for $\sigma = 0.4, 0.6$. Furthermore, the complexity for $\sigma = 0.2$ is the smallest, indicating the strongest decreased effect of improved STDP rule on complexity, and it is the largest for $\sigma = 0.6$, reflecting the strongest increased effect. It is important to note the similar evolutionary processes of modularity and complexity as the momentum factor increases, revealing that the decreased synchronization within the modules yields more modules with smaller size so as to produce higher complexity.

In summary, depending on the momentum factor, the improved STDP rule has different effects on the dynamics of self-organized neuronal network. Compared to the multiplicative STDP rule, the improved STDP rule with $\sigma = 0.1, 0.2, 0.9$ results in a higher network synchronization and local efficiency, less global efficiency, modularity and complexity. However, these changes in the dynamics of self-organized neuronal networks are reversed for $\sigma = 0.6$.

4 Discussion and conclusion

In this paper, we improved the multiplicative STDP rule by adding a momentum term and then studied the evolutionary rate, topological structure and dynamics of self-organized neuronal network with an aim of understanding whether the improved STDP rule optimizes the convergence process and network properties. We first found that the improved STDP rule with suitable momentum factors speeds up the convergence rate with which the global coupled neuronal network evolves into the sparse self-organized structure. Then, using the complex network method, we observed that the

improved STDP rule mostly results in a more sparse, less clustered and modular self-organized neuronal network by affecting the proportion of synaptic weight. Finally, we showed that the improved STDP rule with $\sigma = 0.1, 0.2, 0.9$ strengthens the network synchronization and local efficiency and weakens the global information transmission, modularity and network complexity; however, it has the adverse effect on these dynamical behaviors for $\sigma = 0.6$.

The modulation of chemical synapse is crucial to natural properties of neural system such as the learning and memory, growing and aging [19,23,35,48]. The previous study also suggested that the cellular networks in the adult brain are continually remodeled [2,3,12]. The rate with which the synaptic connections change according to the neural signals has a great effect on the modulation and is also important for high efficiency of information transmission in the neural system. Compared to the multiplicative STDP rule, the improved STDP rule with suitable momentum factors significantly increases the evolutionary rate of neuronal networks such that it optimizes the feedback between neural signals and chemical synapses. Therefore, the improved STDP rule may be more helpful for the higher efficiency of information transmission during the biological feedback process.

The brain networks at all scales have the common properties of sparsity and clusters [3,15]. The improved STDP rule induces the more sparse self-organized neuronal network than the multiplicative STDP rule, which, on the one hand, optimizes the redundant chemical synaptic connections and, on the other hand, increases the long-distance connections between neurons and thus increases the energy cost of information transmission. Combining with the dual effects of improved STDP rule on clustering coefficient, it is hard to identify whether the improved STDP rule results in a more economical and beneficial neuronal network than the multiplicative STDP rule. Therefore, the dynamics of self-organized neuronal network should be considered. It is clear that depending on the momentum factors, the improved STDP rule either strengthens the network synchronization or weakens it. The high network synchronization not only increases the efficiency of information transmission in local loops or global network, but is also related to the brain disorders such as epileptic seizure [21,62]. The optimal synchronization ensures the high

efficiency of information transmission between neurons at low connection cost. Apparently, the improved STDP rule with $\sigma = 0.6$ results in a highest global efficiency (see Fig. 8b), reflecting that the improved STDP rule contributes to the higher efficiency of information transfer across the stable self-organized neuronal network.

The real complex network in the neural system should have the optimal balance between functional segregation and integration which yields the high complex dynamics [3,59]. It is observed that the improved STDP rule with $\sigma = 0.6$ not only induces the highest modularity, but also produces the largest network complexity, reflecting the higher functional segregation but also the optimal balance between functional segregation and integration. Combining with the largest global efficiency of neural information transmission, it is reasonable to claim the optimal structure of self-organized neuronal network which is resulted from the improved STDP rule with $\sigma = 0.6$.

It should be noted that compared to the multiplicative STDP rule, the improved STDP rule with $\sigma = 0.2, 0.6$ induces the most significant changes in the dynamics of neuronal network (Figs. 7, 8, 9). Thus it is reasonable to suspect that the differences between topological structures for $\sigma = 0.2, 0.6$ and $\sigma = 0.0$ are most significant. However, the complex network indices provide insufficient evidence to support the suspect (Fig. 5). In fact, the relationship between structure and dynamics of complex network has been a crucial challenge in neuroscience [53], and the complex network method based on the nodes and edges also has shown the shortcomings in characterizing the intrinsic relationship between network structure and dynamics. In future, the more quantitative methods are required to intrinsically investigate how the network structure decides the dynamics.

In conclusion, the improved STDP rule not only is helpful for decreasing the energy cost during the modulating process of chemical synapses underlying the neural signals, but also contributes to the optimal neuronal network structure with the highest global efficiency and the best combination between functional segregation and integration.

Acknowledgements We wish to acknowledge the financial supports from National Natural Science Foundation of China (Grant Nos. 11272242, 11472202).

Appendix 1: Complex network indices

Node degree

The node degree in directed weighted network is calculated as [40]:

$$k = \frac{1}{n} \sum_{i \in N} k_i = \frac{1}{n} \sum_{i \in N} \sum_{j \in N} (w_{ij} + w_{ji}), \tag{7}$$

where N is the set of all nodes and n is the total number of nodes. The w_{ij} is the synaptic weight from nodes j to i , which is not necessarily equal to w_{ji} .

Clustering coefficient

The local clustering coefficient of node i in directed weighted network is defined as [8]:

$$C_i = \frac{\sum_{j,h \in N, i \neq j \neq h} \left(w_{ij}^{\frac{1}{3}} + w_{ji}^{\frac{1}{3}} \right) \left(w_{ih}^{\frac{1}{3}} + w_{hi}^{\frac{1}{3}} \right) \left(w_{jh}^{\frac{1}{3}} + w_{hj}^{\frac{1}{3}} \right)}{2[k_i(k_i - 1) - 2k_i^{\leftrightarrow}]}, \tag{8}$$

where $k_i^{\leftrightarrow} = \sum_{j \neq i} w_{ij} w_{ji}$ is the number of bilateral edges between node i and its neighbors. The mean clustering coefficient of the network is:

$$C = \frac{1}{n} \sum_{i \in N} C_i. \tag{9}$$

Network efficiency

In undirected weighted network, the global efficiency is defined as [40]:

$$E_{\text{global}}^w = \frac{1}{n} \sum_{i \in N} E_i^w = \frac{1}{n} \sum_{i \in N} \frac{\sum_{j \in N, i \neq j} (d_{ij}^w)^{-1}}{n - 1}, \tag{10}$$

where d_{ij}^w represents the shortest path between nodes i and j .

The local efficiency is defined as [40]:

$$E_{\text{loc}}^w = \frac{1}{2} \sum_{i \in N} \frac{\sum_{j,h \in N} \left(w_{ij} w_{ih} [d_{jh}^w(N_i)]^{-1} \right)^{1/3}}{k_i(k_i - 1)}, \tag{11}$$

where the $d_{jh}(N_i)$ is the length of the shortest path between nodes j and h , that only contains the neighbor of node i .

Modularity

The modularity in directed weighted network is defined as [22]:

$$Q = \frac{1}{l} \sum_{i,j \in N} \left[w_{ij} - \frac{k_i^{\text{in}} k_j^{\text{out}}}{l} \right] \delta_{m_i, m_j}, \tag{12}$$

where $l = \sum_{i,j} w_{ij}$ is the sum of all weights in the network, and the Kronecker delta function δ_{m_i, m_j} is equal to 1 if nodes i and j are in the same modularity.

For undirected weighted network, the modularity is calculated as [40]:

$$Q = \frac{1}{l} \sum_{i,j \in N} \left[w_{ij} - \frac{k_i k_j}{l} \right] \delta_{m_i, m_j}. \tag{13}$$

Appendix 2: Pearson correlation coefficient

The Pearson correlation coefficient is defined as [52]:

$$\rho_{X,Y} = \frac{\sum_{t=1}^T (X(t) - \bar{X})(Y(t) - \bar{Y})}{\sqrt{\sum_{t=1}^T (X(t) - \bar{X})^2 \sum_{t=1}^T (Y(t) - \bar{Y})^2}}, \tag{14}$$

where X and Y are the firing time series for different neurons and \bar{X} and \bar{Y} are the average values corresponding to these time series. The t represents the time point of time series, and T is the total number of time points.

Appendix 3: Network complexity

The complexity of network is measured by Shannon entropy [59]:

$$S = \left(- \sum_{i=1}^m p_i \ln p_i \right) / S_m, \tag{15}$$

where m is the number of bins in the histogram of correlation coefficient and the p_i is the corresponding probability density as shown in Fig. 6c, f and i. The S_m is the Shannon entropy of the uniform distribution and is constantly equal to $\ln m$.

References

- Abbott, L.F., Nelson, S.B.: Synaptic plasticity: taming the beast. *Nat. Neurosci.* **3**, 1178–1183 (2000)
- Alvarez, V.A., Sabatini, B.L.: Anatomical and physiological plasticity of dendritic spines. *Annu. Rev. Neurosci.* **30**, 79–97 (2007)
- Bullmore, E., Sporns, O.: Complex brain networks: graph theoretical analysis of structural and functional systems. *Nat. Rev. Neurosci.* **10**(3), 186–198 (2009)
- Caceres, M.J., Perthame, B.: Beyond blow-up in excitatory integrate and fire neuronal networks: refractory period and spontaneous activity. *J. Theor. Biol.* **350**, 81–89 (2014)
- Cassenaer, S., Laurent, G.: Conditional modulation of spike-timing-dependent plasticity for olfactory learning. *Nature* **482**(7383), 47–52 (2012)
- Dan, Y., Poo, M.M.: Spike timing-dependent plasticity: From synapse to perception. *Physiol. Rev.* **86**(3), 1033–1048 (2006)
- Debanne, D., Gahwiler, B.H., Thompson, S.M.: Long-term synaptic plasticity between pairs of individual ca3 pyramidal cells in rat hippocampal slice cultures. *J. Physiol.* **507**(1), 237–247 (1998)
- Fagiolo, G.: Clustering in complex directed networks. *Phys. Rev. E* **76**(2), 026107 (2007)
- FitzHugh, R.: Impulses and physiological states in theoretical models of nerve membrane. *Biophys. J.* **1**(6), 445–466 (1961)
- Frommke, R.C., Dan, Y.: Spike-timing-dependent synaptic modification induced by natural spike trains. *Nature* **416**(6879), 433–438 (2002)
- Gan, C.B., Perc, M., Wang, Q.Y.: Delay-aided stochastic multiresonances on scale-free Fitzhugh–Nagumo neuronal networks. *Chin. Phys. B* **19**(4), 040508 (2010)
- Grutzendler, J., Kasthuri, N., Gan, W.B.: Long-term dendritic spine stability in the adult cortex. *Nature* **420**(6917), 812–816 (2002)
- Gu, H., Pan, B., Li, Y.: The dependence of synchronization transition processes of coupled neurons with coexisting spiking and bursting on the control parameter, initial value, and attraction domain. *Nonlinear Dyn.* **82**(3), 1191–1210 (2015)
- He, B.J., Zempel, J.M., Snyder, A.Z., Raichle, M.E.: The temporal structures and functional significance of scale-free brain activity. *Neuron* **66**(3), 353–69 (2010)
- He, Y., Chen, Z.J., Evans, A.C.: Small-world anatomical networks in the human brain revealed by cortical thickness from mri. *Cereb. Cortex* **17**(10), 2407–2419 (2007)
- van den Heuvel, M.P., Stam, C.J., Boersma, M., Hulshoff Pol, H.E.: Small-world and scale-free organization of voxel-based resting-state functional connectivity in the human brain. *Neuroimage* **43**(3), 528–539 (2008)
- Hosaka, R., Araki, O., Ikeguchi, T.: Stdp provides the substrate for igniting synfire chains by spatiotemporal input patterns. *Neural Comput.* **20**(2), 415–435 (2008)
- Kato, H., Kimura, T., Ikeguchi, T.: Emergence of self-organized structures in a neural network using two types of STDP learning rules. In: *Proceedings of 2007 International Symposium on Nonlinear Theory and its Applications*, pp. 429–432 (2007)
- Kaul, R.A., Syed, N.I., Fromherz, P.: Neuron-semiconductor chip with chemical synapse between identified neurons. *Phys. Rev. Lett* **92**(3), 038102 (2004)
- Kim, S.J., Linden, D.J.: Ubiquitous plasticity and memory storage. *Neuron* **56**(4), 582–592 (2007)
- Kudela, P., Franaszczuk, P.J., Bergey, G.K.: Changing excitation and inhibition in simulated neural networks: effects on induced bursting behavior. *Biol. Cybern.* **88**(4), 276–85 (2003)
- Leicht, E.A., Newman, M.E.: Community structure in directed networks. *Phys. Rev. Lett* **100**(11), 118703 (2008)
- Lewis, D.A., Volk, D.W., Hashimoto, T.: Selective alterations in prefrontal cortical gaba neurotransmission in schizophrenia: a novel target for the treatment of working memory dysfunction. *Psychopharmacol.* **174**(1), 143–150 (2004)
- Li, F., Ma, J.: Pattern selection in network of coupled multi-scroll attractors. *PLoS One* **11**(4), e0154282 (2016)
- Li, J., Liu, S., Liu, W., Yu, Y., Wu, Y.: Suppression of firing activities in neuron and neurons of network induced by electromagnetic radiation. *Nonlinear Dyn.* **83**(1–2), 801–810 (2016)
- Li, X., Zhang, J., Small, M.: Self-organization of a neural network with heterogeneous neurons enhances coherence and stochastic resonance. *Chaos* **19**(1), 013126 (2009)
- Lin, P., Sun, J., Yu, G., Wu, Y., Yang, Y., Liang, M., Liu, X.: Global and local brain network reorganization in attention-deficit/hyperactivity disorder. *Brain Imaging Behav.* **8**(4), 558–69 (2014)
- Lin, P., Yang, Y., Jovicich, J., De Pisapia, N., Wang, X., Zuo, C.S., Levitt, J.J.: Static and dynamic posterior cingulate cortex nodal topology of default mode network predicts attention task performance. *Brain Imaging Behav.* **10**(1), 212–225 (2016)
- Ma, J., Hu, B., Wang, C., Jin, W.: Simulating the formation of spiral wave in the neuronal system. *Nonlinear Dyn.* **73**(1–2), 73–83 (2013)
- Ma, J., Qin, H., Song, X., Chu, R.: Pattern selection in neuronal network driven by electric autapses with diversity in time delays. *Int. J. Mod. Phys. B* **29**(01), 1450239 (2015)
- Ma, J., Song, X., Tang, J., Wang, C.: Wave emitting and propagation induced by autapse in a forward feedback neuronal network. *Neurocomputing* **167**, 378–389 (2015)
- Ma, J., Tang, J.: A review for dynamics of collective behaviors of network of neurons. *Sci. China Technol. Sc.* **58**(12), 2038–2045 (2015)
- Markram, H.: Regulation of synaptic efficacy by coincidence of postsynaptic apss and epsps. *Science* **275**(5297), 213–215 (1997)
- Markram, H., Gerstner, W., Sjostrom, P.J.: A history of spike-timing-dependent plasticity. *Front. Synaptic Neurosci.* **3**(23), 1–24 (2011)

35. Mongillo, G., Barak, O., Tsodyks, M.: Synaptic theory of working memory. *Science* **319**(5869), 1543–1546 (2008)
36. Morelli, L.G., Abramson, G., Kuperman, M.N.: Associative memory on a small-world neural network. *Eur. Phys. J. B* **38**(3), 495–500 (2004)
37. Nishimura, Y., Perlmutter, S.I., Eaton, R.W., Fetz, E.E.: Spike-timing-dependent plasticity in primate corticospinal connections induced during free behavior. *Neuron* **80**(5), 1301–9 (2013)
38. Perc, M.: Thoughts out of noise. *Eur. J. Phys.* **27**(2), 451 (2006)
39. Perc, M.: Effects of small-world connectivity on noise-induced temporal and spatial order in neural media. *Chaos Soliton Fract.* **31**(2), 280–291 (2007)
40. Rubinov, M., Sporns, O.: Complex network measures of brain connectivity: uses and interpretations. *Neuroimage* **52**(3), 1059–69 (2010)
41. Sadeghi, B.: A bp-neural network predictor model for plastic injection molding process. *J. Mater. Process. Tech.* **103**(3), 411–416 (2000)
42. Serrano-Gotarredona, T., Masquelier, T., Prodromakis, T., Indiveri, G., Linares-Barranco, B.: STDP and STDP variations with memristors for spiking neuromorphic learning systems. *Front. Neurosci.* **7**, 2 (2013)
43. Shin, C.W., Kim, S.: Self-organized criticality and scale-free properties in emergent functional neural networks. *Phys. Rev. E* **74**(4), 045101 (2006)
44. Shiyong, H., Haganir, R.L., Alfredo, K.: Adrenergic gating of hebbian spike-timing-dependent plasticity in cortical interneurons. *J. Neurosci.* **33**(32), 13171–13178 (2013)
45. Song, S., Miller, K.D., Abbott, L.F.: Competitive hebbian learning through spike-timing-dependent synaptic plasticity. *Nat. Neurosci.* **3**(9), 919–926 (2000)
46. Sporns, O., Tononi, G., Edelman, G.M.: Theoretical neuroanatomy: relating anatomical and functional connectivity in graphs and cortical connection matrices. *Cereb. Cortex* **10**(2), 127–141 (2000)
47. Sun, X., Shi, X.: Effects of channel blocks on the spiking regularity in clustered neuronal networks. *Sci. China Technol. Sc.* **57**(5), 879–884 (2014)
48. Toth, M.L., Melentijevic, I., Shah, L., Bhatia, A., Lu, K., Talwar, A., Naji, H., Ibanez-Ventoso, C., Ghose, P., Jevince, A., et al.: Neurite sprouting and synapse deterioration in the aging caenorhabditis elegans nervous system. *J. Neurosci.* **32**(26), 8778–8790 (2012)
49. Wang, Q., Zhang, H., Perc, M., Chen, G.: Multiple firing coherence resonances in excitatory and inhibitory coupled neurons. *Commun. Nonlinear Sci.* **17**(10), 3979–3988 (2012)
50. Wang, R., Li, J., Du, M., Lei, J., Wu, Y.: Transition of spatiotemporal patterns in neuronal networks with chemical synapses. *Commun. Nonlinear Sci.* **40**, 80–88 (2016)
51. Wang, R., Li, J., Wang, L., Yang, Y., Lin, P., Wu, Y.: Application of complex network method to spatiotemporal patterns in a neuronal network. *Phys. A* **463**, 219–230 (2016)
52. Wang, R., Zhang, Z.Z., Ma, J., Yang, Y., Lin, P., Wu, Y.: Spectral properties of the temporal evolution of brain network structure. *Chaos* **25**(12), 7641–7646 (2015)
53. Wang, Z., Dai, Z., Gong, G., Zhou, C., He, Y.: Understanding structural-functional relationships in the human brain: a large-scale network perspective. *Neuroscientist* **21**(3), 290–305 (2014)
54. Wolters, A., Sandbrink, F., Schlottmann, A., Kunesch, E., Stefan, K., Cohen, L.G., Benecke, R., Classen, J.: A temporally asymmetric Hebbian rule governing plasticity in the human motor cortex. *J. Neurophysiol.* **89**(5), 2339–2345 (2003)
55. Yu, H., Guo, X., Wang, J., Deng, B., Wei, X.: Spike coherence and synchronization on Newman-Watts small-world neuronal networks modulated by spike-timing-dependent plasticity. *Phys. A* **419**, 307–317 (2015)
56. Yu, H., Guo, X., Wang, J., Liu, C., Deng, B., Wei, X.: Adaptive stochastic resonance in self-organized small-world neuronal networks with time delay. *Commun. Nonlinear Sci.* **29**(1–3), 346–358 (2015)
57. Zhang, H., Wang, Q., Perc, M., Chen, G.: Synaptic plasticity induced transition of spike propagation in neuronal networks. *Commun. Nonlinear Sci.* **18**(3), 601–615 (2013)
58. Zhang, J., Zhou, C., Xu, X., Small, M.: Mapping from structure to dynamics: a unified view of dynamical processes on networks. *Phys. Rev. E* **82**(2), 026116 (2010)
59. Zhao, M., Zhou, C., Chen, Y., Hu, B., Wang, B.H.: Complexity versus modularity and heterogeneity in oscillatory networks: combining segregation and integration in neural systems. *Phys. Rev. E* **82**(4), 046225 (2010)
60. Zhao, Z., Jia, B., Gu, H.: Bifurcations and enhancement of neuronal firing induced by negative feedback. *Nonlinear Dyn.* **86**(3), 1549–1560 (2016)
61. Zheng, P., Dimitrakakis, C., Triesch, J.: Network self-organization explains the statistics and dynamics of synaptic connection strengths in cortex. *PLoS Comput. Biol* **9**(1), e1002848 (2013)
62. Zhou, C., Zemanova, L., Zamora-Lopez, G., Hilgetag, C.C., Kurths, J.: Structure-function relationship in complex brain networks expressed by hierarchical synchronization. *New J. Phys.* **9**(6), 178–178 (2007)